

THERMAL NON-EQUILIBRIUM EFFECTS ON THE FLOWFIELD STRUCTURE OF HYPERSONIC BACKWARD-FACING STEP FLOW

Paulo H. M. Leite and Wilson F. N. Santos

*Combustion and Propulsion Laboratory (LCP), National Institute for Space Research (INPE),
Cachoeira Paulista, SP, 12630-000, BRAZIL, wilson@lcp.inpe.br, <http://www.lcp.inpe.br>*

Keywords: DSMC, Hypersonic Flow, Rarefield Flow, Non-Equilibrium Effects, Backward-Facing Step, Reentry.

Abstract. An exploratory computational investigation was made on backward-facing steps in a rarefied hypersonic flow. The effect of the step back-face height on the thermal non-equilibrium was examined by employing the Direct Simulation Monte Carlo (DSMC) method. Results for the non-equilibrium between rotational temperature, vibrational temperature, “parallel” temperature, “normal” temperature, and translational temperature were presented and discussed at length. “Parallel” temperature and “normal” temperature are kinetic temperatures associated with x and y coordinate directions in the flowfield. Results showed that the flowfield is in thermal non-equilibrium in the boundary layer and in the shock-wave layer. In contrast, thermal equilibrium was verified at the vicinity of the step base. It was also found that entropy generation regions are related to the thermal non-equilibrium regions in the flowfield.

1. INTRODUCTION

The development of aerospace technology has generated a strong demand on research associated with rarefied gas dynamics. Usually, the development of space vehicles in this area involves reentry type vehicles, exploratory interplanetary vehicles, etc. These space vehicles, which operate in the higher atmosphere at hypersonic speeds, are generally designed with contour discontinuities, such as cavities, gaps or steps. The presence of these discontinuities in modern aerodynamics configurations occurs as a desired or undesired design feature, although a smooth aerodynamic shape of the surface is attempted. The hypersonic flow over backward-facing steps involves flow separation and reattachment. The separating and reattaching flow phenomena may affect locally thermal and aerodynamic loads that may exceed the ones of a smooth surface. Therefore, in order to operate safely, these loads have to be predicted correctly.

Many experimental and theoretical studies (Charwat et al., 1961; Donaldson, 1967; Gai and Milthorpe, 1995; Gai et al., 1989; Grotowsky and Ballmann, 2000; Loth et al., 1992; Rom and Seginer, 1964; Scherberg and Smith, 1967; Shang and Korkegi, 1968) have been conducted in order to understand the physical aspects of subsonic and supersonic flows past to this type of discontinuity, characterized by a sudden change on the surface slope. For the purpose of this introduction, it will be sufficient to describe only a few of these studies.

Rom and Seginer (1964) have investigated experimentally the heat-transfer rate on a 2-D backward-facing step in a laminar supersonic flow, corresponding to Mach number in the range of 1.5 to 2.5, and Reynolds number in the range from 10^3 to 10^5 . Results indicated that the heat-transfer rates changed with the distance behind the step. In addition, it was found that the heat transfer rates depended on the ratio of the boundary-layer thickness at the separation to the step height.

Data presented by Charwat et al. (1961) indicated that flow which separates from an isolated backward-facing step impinges on the wall approximately a distance of seven times the step height downstream of the step if the boundary layer is laminar, and approximately five times the step height downstream for a turbulent boundary layer.

Gai and Milthorpe (1995) presented experimental and computational results of a high enthalpy flow over a blunted-stepped cone. Basically, an axisymmetric backward-facing step of height of 3 mm and 6 mm located at a distance of 101 mm from the nose. The analysis showed that the heat transfer rate was typical of that in a separated flow, i.e., a sudden fall in heat transfer very near the step and then a gradual increase beyond it. The experimental data showed a decrease in heat transfer rate after reattachment, whereas the numerical prediction exhibited a plateau for a considerable distance.

Grotowsky and Ballmann (2000) investigated laminar hypersonic flow over forward- and backward-facing steps by employing Navier-Stokes equations. The hypersonic flow over the steps were simulated by considering freestream Mach number of 8, Reynolds number of the order of 10^8 and an altitude of 30 km. According to them, the computational results presented a good agreement with the experimental data available in the literature. They also pointed out that the quantitative comparison exhibited major differences for the wall heat flux, probably due to the difficulty in how to measure accurately.

According to the current literature, the flow past to backward-facing steps has been experimentally and theoretically studied in the past at subsonic and supersonic speeds. Nevertheless, not much data exists at hypersonic flow past to steps related to the severe aerothermodynamic environment associated with a reentry vehicle. In this context, a numerical study on backward-facing steps, situated in a rarefied hypersonic flow, has been examined by Leite and Santos (2009a) by employing the DSMC method. The work was motivated by the interest in investigating the step-height effects on the flowfield structure. The primary emphasis was to examine

the sensitivity of velocity, density, pressure and temperature fields with respect to step-height variations of such backward-facing steps. The analysis showed that the hypersonic flow past to backward-facing steps was characterized by a strong expansion wave around de corner of the steps, which influenced the downstream separation region. It was found that the recirculation region relies on the back-face height. The analysis also showed that disturbances downstream the steps depend on changes in the back-face height of the steps.

Leite and Santos (2009b) have extended the previous analysis (Leite and Santos, 2009a) by investigating the impact of the back-face height on the aerodynamic surface quantities. The primary goal was to assess the sensitivity of the heat transfer, pressure and skin friction coefficients to variations on the back-face height of the steps. It was found that changes on the step height affected the aerodynamic surface quantities a distance of a few mean free paths upstream of it. In addition, heat transfer, pressure, and skin friction coefficients were affected downstream the steps due to changes on the rear-face height of the steps.

The present investigation was undertaken in an attempt to expand further the previous analysis (Leite and Santos, 2009a) by investigating the impact of the step back-face height on the thermal non-equilibrium. In this fashion, the focus of this study is to assess the sensitivity of kinetic translational temperature T_T , rotational temperature T_R , vibrational temperature T_V and the kinetic temperatures associated with x and y coordinate directions in the flowfield, i.e., T_X and T_Y , to variations on the step back-face height. In addition, the investigation focuses on the physical aspects of hypersonic flow past to steps related to the severe aerothermodynamic environment associated to a reentry vehicle in the transition flow regime. In doing so, the Direct Simulation Monte Carlo (DSMC) method will be employed to calculate the hypersonic two-dimensional flow over the steps.

2. GEOMETRY DEFINITION

The definition of the backward-facing step geometry follows that one presented in the previous study, Leite and Santos (2009a). It was assumed that the step back-face height h is much smaller than the nose radius R of a reentry capsule, i.e., $h/R \ll 1$. Therefore, discontinuities on the surface of a reentry vehicle are considered herein as a hypersonic flow over a flat plate with a backward-facing step positioned far from the stagnation point. A schematic representation of the geometric model is illustrated in Figure 1(a).

Based on Fig. 1(a), M_∞ represents the freestream Mach number, h is the back-face height, L_u stands for the upstream flat-plate length, and L_d for the downstream flat-plate length. It was considered that the flat plate is infinitely long but only the total length L is examined. It was assumed a back-face height h of 0, 3, 6, and 9 mm, which correspond to h/λ_∞ of 0, 3.23, 6.46 and 9.69, L_u/λ_∞ of 50 and L_d/λ_∞ of 120, where λ_∞ is the freestream molecular mean free path. The particular case of $h/\lambda_\infty = 0$ corresponds to the flat-plate case free of surface discontinuities. Therefore, the flat-plate case works as a benchmark for the cases with steps.

2.1 COMPUTATIONAL METHOD AND PROCEDURE

The degree of departure of a flow from continuum is indicated by the flow Knudsen number, $Kn = \lambda/l$, where λ is the molecular mean free path and l is the characteristic length of the flow. Traditionally, flows are divided into four regimes (Schaff and Chambre, 1958): $Kn < 0.01$, continuum flow regime, $0.01 < Kn < 0.1$, slip flow regime, $0.1 < Kn < 10$, transition flow regime, and $Kn > 10$, free molecular flow regime or collisionless flow regime.

Based on these flow regimes, the choice of the numerical approach to be used in order to model rarefied non-equilibrium flows greatly relies on the extent of flow rarefaction. For near-continuum flows, it is usually sufficient to take into account the effects of rarefaction through the

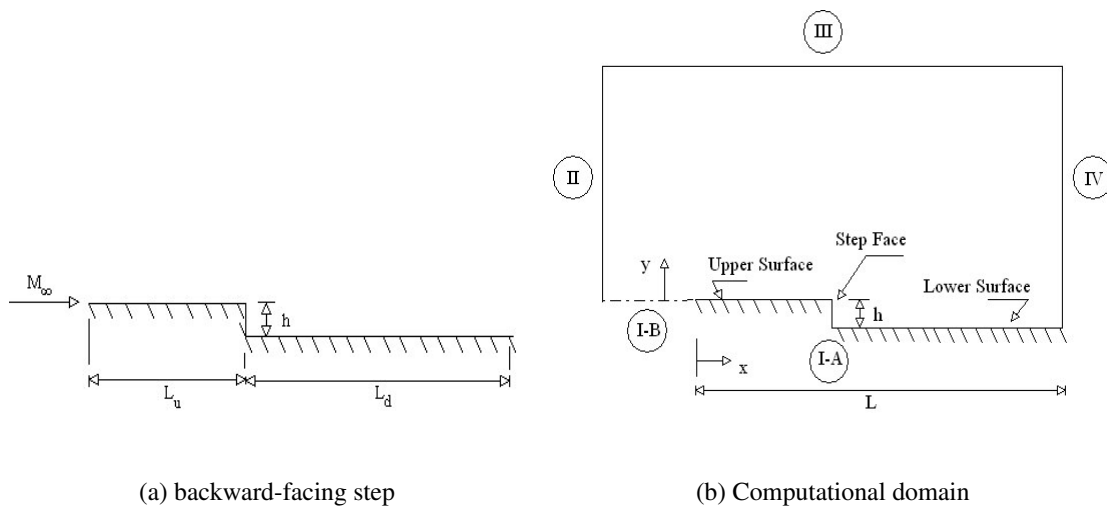


Figure 1: Drawing illustrating (a) the backward-facing step and (b) the computational domain.

boundary conditions of slip velocity and temperature jump on the surface. The Navier-Stokes equations, commonly used with these boundary conditions, can be derived from the Boltzmann equation under the assumption of small deviation of the distribution function from equilibrium. Nevertheless, the Navier-Stokes equations became unsuitable for studying rarefied flows where the distribution function becomes considerable in non-equilibrium.

In order to study rarefied flow with a significant degree of non-equilibrium, the Direct Simulation Monte Carlo (DSMC) method (Bird, 1994) is usually employed. The DSMC method has become the most common computational technique for modeling complex transition flows of engineering interest. The DSMC method simulates real gas flows with various physical processes by using a computer to track the trajectory of simulated particles, where each simulated particle represents a fixed number of real gas particles. The simulated particles are allowed to move and collide, while the computer stores their position coordinates, velocities and other physical properties such as internal energy.

The particle evolution is divided into two independent phases during the simulation: the movement phase and the collision phase. In the movement phase, all particles are moved over distances appropriate to a short time interval, time step, and some of them interact with the domain boundaries in this time interval. Particles that strike the solid wall would reflect according to the appropriate gas-surface interaction model; specular, diffuse or a combination of these. In the collision phase, intermolecular collisions are performed according to the theory of probability without time being consumed. In this way, the intermolecular collisions are uncoupled to the translational molecular motion over the time step used to advance the simulation. The simulation is always calculated as unsteady flow, however, a steady-flow solution is obtained as the large time state of the simulation.

In the present account, the molecular collision kinetics are modeled by using the variable hard sphere (VHS) molecular model (Bird, 1981), and the no time counter (NTC) collision sampling technique (Bird, 1989). The VHS model employs the simple hard sphere angular scattering law so that all directions are equally possible for post-collision velocity in the center-of-mass frame of reference. Nevertheless, the collision cross section depends on the relative speed of colliding molecules. The mechanics of the energy exchange processes between kinetic and internal modes for rotation and vibration are controlled by the Borgnakke-Larsen statisti-

cal model (Borgnakke and Larsen, 1975). The essential feature of this model is that part of collisions is treated as completely inelastic, and the remainder of the molecular collisions is regarded as elastic. Simulations are performed using a non-reacting gas model, consisting of 76.3% of N_2 and 23.7% of O_2 . The vibrational temperature is controlled by the distribution of energy between the translational and rotational modes after an inelastic collision. The probability of an inelastic collision determines the rate at which energy is transferred between the translational and internal modes after an inelastic collision. For a given collision, the probabilities are designated by the inverse of the relaxation numbers, which correspond to the number of collisions necessary, on average, for a molecule undergoes relaxation. The rates of rotational and vibrational relaxation are dictated by collision numbers Z_R and Z_V , respectively. Relaxation collision numbers of 5 and 50 were used for the calculations of rotation and vibration, respectively.

2.2 COMPUTATIONAL DOMAIN AND GRID

In order to implement the particle collisions, the flowfield around the backward-facing step is divided into an arbitrary number of regions, which are subdivided into computational cells. The cells are further subdivided into subcells, two subcells/cell in each coordinate direction. In this way, collision partners are selected from the same subcell for the establishment of the collision rate, while the cell provides a convenient reference for the sampling of the macroscopic gas properties. The computational domain used for the calculation is made large enough so that body disturbances do not reach the upstream and side boundaries, where freestream conditions are specified. A schematic view of the computational domain is depicted in Fig. 1(b).

According to this figure, side I-A is defined by the body surface. Diffuse reflection with complete thermal accommodation is the condition applied to this side. In a diffuse reflection, the molecules are reflected equally in all directions, and the final velocity of the molecules is randomly assigned according to a half-range Maxwellian distribution determined by the wall temperature. Side I-B is a plane of symmetry, where all flow gradients normal to this plane are zero. At the molecular level, this plane is equivalent to a specular reflecting boundary. Sides II and III are the freestream sides through which simulated molecules enter and exit. Finally, the flow at the downstream outflow boundary, side IV, is predominantly supersonic and vacuum condition is specified (Bird, 1994). At this boundary, simulated molecules can only exit.

The numerical accuracy in DSMC method depends on the cell size chosen, on the time step as well as on the number of particles per computational cell. In the DSMC code, the linear dimensions of the cells should be small in comparison with the scale length of the macroscopic flow gradients normal to the streamwise directions, which means that the cell dimensions should be the order of or smaller than the local mean free path (Alexander et al., 1998, 2000). The time step should be chosen to be sufficiently small in comparison with the local mean collision time (García and Wagner, 2000; Hadjiconstantinou, 2000). In general, the total simulation time, discretized into time steps, is based on the physical time of the real flow. Finally, the number of simulated particles has to be large enough to make statistical correlations between particles significant. These effects were investigated in order to determine the number of cells and the number of particles required to achieve grid independent solutions. Grid independence was tested by running the calculations with half and double the number of cells in the coordinate directions compared to a standard grid. Solutions (not shown) were nearly identical for all grids used and were considered fully grid independent. A discussion of these effects on the aerodynamic surface quantities is described in detail by Leite (2009).

3. FREESTREAM AND FLOW CONDITIONS

Freestream conditions employed in the present calculations are those given by Leite and Santos (2009a), and the gas properties follow those given by Bird (1994). For completeness, Tables 1 and 2 tabulate the freestream conditions and the gas properties, respectively. Referring to Table 1, U_∞ , T_∞ , p_∞ , ρ_∞ , μ_∞ , n_∞ and λ_∞ stand respectively for velocity, temperature, pressure, density, viscosity, number density and the molecular mean free path. Based on Table 2, X , m , d and ω account respectively for mass, molecular diameter and viscosity index.

U_∞ (m/s)	T_∞ (K)	p_∞ (N/m ²)	ρ_∞ (kg/m ³)	μ_∞ (Ns/m ²)	n_∞ (m ⁻³)	λ_∞ (m)
7456	219.69	5.582	8.753×10^{-5}	1.455×10^{-5}	1.8192×10^{21}	9.285×10^{-4}

Table 1: Freestream flow conditions

	X	m (kg)	d (m)	ω
O_2	0.237	5.312×10^{-26}	4.01×10^{-10}	0.77
N_2	0.763	4.650×10^{-26}	4.11×10^{-10}	0.74

Table 2: Gas properties

The freestream velocity U_∞ , assumed to be constant at 7456 m/s, corresponds to a freestream Mach number M_∞ of 25. The wall temperature T_W is assumed constant at 880 K. This temperature is chosen to be representative of the surface temperature near the stagnation point of a reentry capsule and is assumed to be uniform on the backward-facing-step surface. It is important to mention that the surface temperature is low compared to the stagnation temperature T_O of the air, i.e., $T_W/T_O = 0.013$. This assumption seems reasonable since practical surface material will probably be destroyed if surface temperature is allowed to approach the stagnation temperature.

By assuming the back-face height h as the characteristic length, the Knudsen number Kn_h corresponds to 0.3095, 0.1548 and 0.1032 for height h of 3, 6 and 9 mm, respectively. Finally, the Reynolds number Re_h , also based on the back-face height h and on conditions in the undisturbed stream, is around 136, 272, and 409 for height h of 3, 6 and 9 mm, respectively.

4. COMPUTATIONAL RESULTS AND DISCUSSION

It is firmly established that each law of thermodynamics is associated with the definition of a new system property. For instance, the internal energy is related to the first law, and entropy to the second law. In this context, the zeroth law defines the thermodynamic property called “temperature”.

Thermodynamic temperature is defined classically in terms of a reversible engine operating between two reservoirs by the following relation (Bejan, 1988),

$$\frac{T_1}{T_2} = \frac{Q_1}{Q_2} \quad (1)$$

where T is the temperature and Q is the amount of heat transferred.

Heat may be transferred either by conduction or radiation process. On one hand, the conduction process is controlled by the translational energy of the molecules. On the other hand, radiation occurs by means of rotational, vibrational or electronic transitions, and is thus related to the corresponding energy distributions. According to the arguments of statistical mechanics, the energy of a gas is described by distribution functions for the various modes of energy storage. In order to characterize a distribution function by a single parameter, the temperature, each degree of freedom of the gas must be internally equilibrated. Nevertheless, the statistical description does not require equilibrium between modes of energy storage (Mates and Weatherston, 1965). In this way, one may speak of a translational temperature, a rotational temperature, a vibrational temperature, and so forth.

For a diatomic or polyatomic gas in complete thermodynamic equilibrium, the translational temperature is equal to the temperature related to the internal modes, i.e., rotational, vibrational or electronic temperatures, and it is identified as thermodynamic temperature. When the equilibrium is disturbed, relaxation processes arise in the system that attempt to return it to the state of the total statistical equilibrium. In diatomic or polyatomic gas, these are processes which results in the establishment of equilibrium with respect to individual degrees of molecular freedom such as translational, rotational, vibrational or electronic. Conversely, in a thermodynamic non-equilibrium gas, an overall temperature is defined as the weighted mean of the translational and internal temperatures (Bird, 1994) as being,

$$T_{OV} = \frac{\zeta_T T_T + \zeta_R T_R + \zeta_V T_V}{\zeta_T + \zeta_R + \zeta_V} \quad (2)$$

where ζ is the degree of freedom and subscript T , R and V stand for translation, rotation and vibration, respectively.

In the DSMC, translational, rotational, and vibrational temperatures are obtained to each cell in the computational domain by the following equations,

$$T_T = \frac{1}{3k} \sum_{j=1}^N \frac{(mc'^2)_j}{N} \quad (3)$$

$$T_R = \frac{2 \bar{\varepsilon}_R}{k \zeta_R} \quad (4)$$

$$T_V = \frac{\Theta_V}{\ln(1 + k\Theta_V/\bar{\varepsilon}_V)} \quad (5)$$

where k is the Boltzmann constant, c' is the thermal velocity of the molecules, Θ_V is the characteristic temperature of vibration, and $\bar{\varepsilon}_R$ and $\bar{\varepsilon}_V$ are, respectively, rotation and vibration average energies in each cell.

It is also firmly established that a spacecraft entering into the atmosphere at hypersonic speed experiences two important features: (1) the strong shock wave that forms around the vehicle converts part of the kinetic energy of the freestream air molecules into thermal energy, the shock compression leads to strong molecular collisions. This thermal energy is partitioned into increasing the translational kinetic energy of the air molecules, and into exciting other molecular energy states such as rotation and vibration; (2) the low density of the atmosphere

results in small molecular collision rates and, therefore, the thermal process may take place in local non-equilibrium conditions.

Having a clear qualitative picture of the physical features involved in a reentry hypersonic flow, the analysis now focuses on the temperature field on the backward-facing step, which represents one type of discontinuity on the surface of reentry vehicles. In doing so, kinetic temperature profiles for six sections along the upper and lower surfaces of the steps are displayed in Fig. 2. In this set of plots, X represents the distance x normalized by the freestream mean free path λ_∞ , Y the distance y above the upper surface normalized by λ_∞ , Y' the distance $(y + h)$ above the lower surface normalized by the step h , temperature ratio stands for the translational temperature T_T , rotational temperature T_R , vibrational temperature T_V or overall temperature T_{OV} normalized by the freestream temperature T_∞ . Also, filled and empty symbols correspond to kinetic temperature distributions for height h of 3 and 9 mm, respectively. As a base of comparison, the black-solid lines correspond to the kinetic temperature profiles for the flat-plate case. It should be remarked that the step is located at station $X = 50$. Therefore, the first three profiles correspond to the upper surface and the other profiles to the lower surface.

It is apparent from this set of plots that thermodynamic non-equilibrium occurs throughout the shock layer, as shown by the lack of equilibrium of the translational and internal kinetic

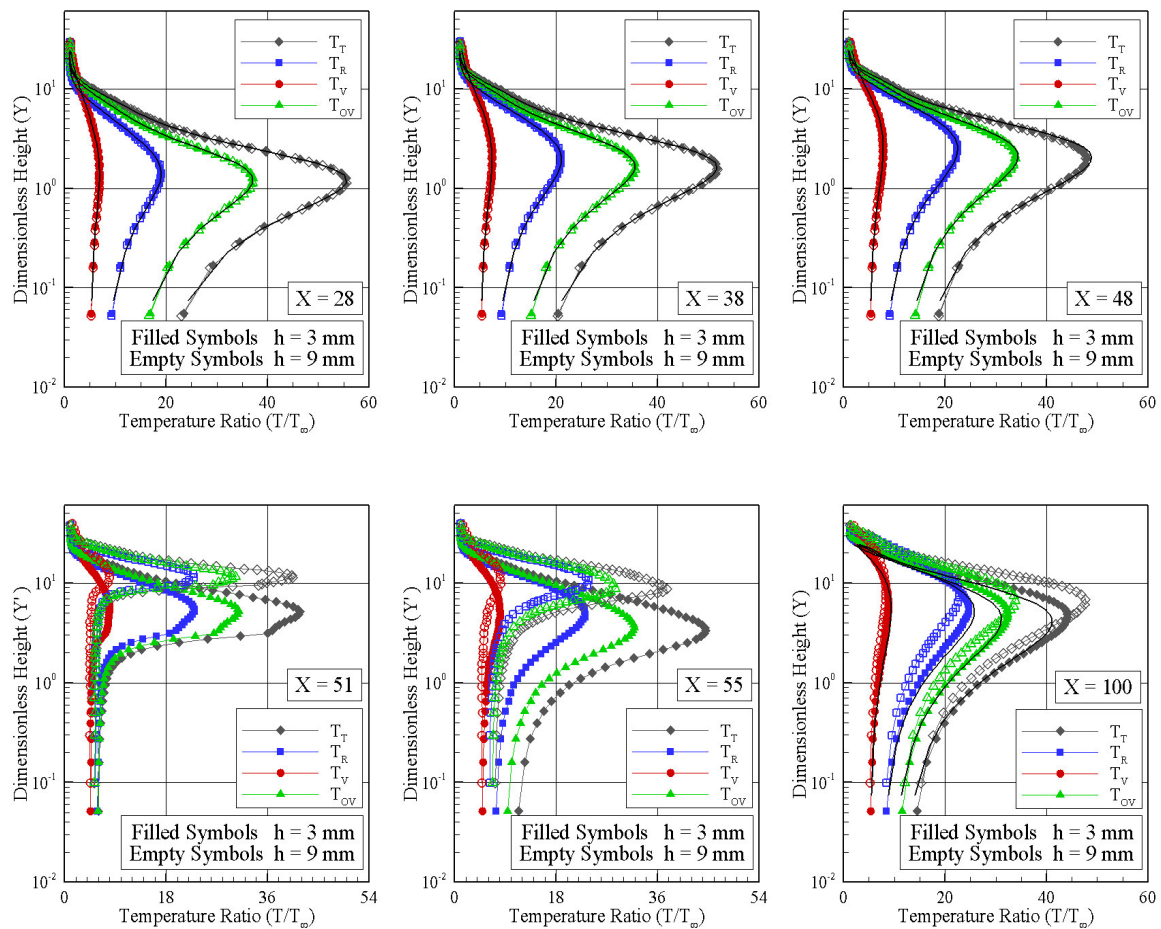


Figure 2: Distribution of kinetic temperature ratio (T/T_∞) profiles along the backward-facing step surface as a function of the height h .

temperatures. Thermal non-equilibrium occurs when the temperatures associated with translational, rotational, and vibrational modes of a polyatomic gas are different.

On examining the temperature profiles on the upper surface, it should be recognized that, in the undisturbed freestream far from the upper surface, $Y \rightarrow \infty$, the translational and internal kinetic temperatures (rotational and vibrational) have the same value and are equal to the thermodynamic temperature. Approaching the upper surface, for instance, $Y \approx 2$, the translational kinetic temperature rises to well above the rotational and vibrational temperatures, and reaches a maximum value that is a function of the section X . Since a large number of collisions is needed to excite molecules vibrationally from the ground state to the upper state, the vibrational temperature is seen to increase much more slowly than rotational temperature. The translational kinetic temperature rise results from the essentially bimodal velocity distribution: the molecular sample consisting of mostly undisturbed freestream molecules with the molecules that have been affected by the shock and reflected from the step surface. In this manner, the translational kinetic temperature rise is a consequence of the large velocity separation between these two classes of molecules. The bimodal velocity distribution was pointed out by [Liepmann et al. \(1964\)](#).

Still further toward the upper surface, $Y \approx 0$, the translational and internal temperatures decrease, and reach values on the wall that are above the wall temperature $T_W (\approx 4T_\infty)$, resulting in a temperature jump as defined in continuum formulation. In addition, it is also recognized from these plots that, for the step height investigated, kinetic temperature profiles on the upper surface are exactly the same as those presented by the flat-plate case. Therefore, no upstream disturbance is detected due to the presence of the backward-facing steps. Moreover, it is seen that the downstream evolution of the flow along the upper surface displays a smearing tendency of the shock wave due to the displacement of the maximum value for the translational temperature as well as for the overall kinetic temperature.

Turning to the kinetic temperature profiles on the lower surface, it is noticed that the temperature distribution is a function of the step height h . For section $X = 51$, at the vicinity of the back face, which corresponds to the recirculation region, the difference between translational temperature and internal temperatures drastically decreases, and temperatures approach the wall temperature, indicating that the thermodynamic equilibrium is roughly achieved in this region. In addition, for section $X = 100$, therefore far from the back face and from the flow reattachment point, the flow develops again along the surface, and the temperature profiles basically recover the profiles observed for the flat-plate case.

In order to bring out the essential features of the thermal non-equilibrium at the vicinity of the backward-facing steps, effects of the back-face height on the thermal non-equilibrium are highlighted by means of temperature parameters defined as following,

$$\eta_R = 1 - \frac{T_R}{T_T} \quad (6)$$

$$\eta_V = 1 - \frac{T_V}{T_T} \quad (7)$$

$$\eta_X = 1 - \frac{T_X}{T_T} \quad (8)$$

$$\eta_Y = 1 - \frac{T_Y}{T_T} \quad (9)$$

where the subscript X and Y stand, respectively, for translational kinetic temperature associated with x and y coordinate directions, i.e., “parallel” and “normal” temperatures.

Before looking at the problem in more detail, a brief consideration of the parameters η_X and η_Y is in order. The average kinetic energy associated with the thermal or translational motion of a molecule is $m\overline{c^2}/2$, and the specific energy associated with this motion is $e_{tr} = \overline{c^2}/2$. In this way, the translational kinetic temperature is defined by the following expression,

$$\frac{3}{2}kT_{tr} = \frac{1}{2}m\overline{c^2} \quad (10)$$

However, this equation may be rearranged as,

$$k\left(\frac{1}{2}T_{tr,x} + \frac{1}{2}T_{tr,y} + \frac{1}{2}T_{tr,z}\right) = \frac{1}{2}m(\overline{u^2} + \overline{v^2} + \overline{w^2}) \quad (11)$$

Moreover, separate translational kinetic temperatures may be defined for each component associated with the coordinate directions as follows,

$$\begin{aligned} kT_{tr,x} &= m\overline{u^2} \\ kT_{tr,y} &= m\overline{v^2} \\ kT_{tr,z} &= m\overline{w^2} \end{aligned} \quad (12)$$

Therefore, the departure of these component temperatures from T_{tr} provides a measure of the degree of translational non-equilibrium. In the present account, T_{tr} , $T_{tr,x}$, and $T_{tr,y}$ are defined by T_T , T_X , and T_Y , respectively.

The distribution of non-equilibrium between rotational and translational temperatures, η_R , is displayed in Fig. 3 for six sections along the upper and lower surfaces of the steps. For comparison purpose, this group of plots presents the parameter η_R for the flat-plate case, i.e., a flat plate without a step. According to these plots, at sections X of 28, 38 and 48, it is seen that η_R profiles for the steps basically follow the same behavior as that presented by the flat-plate case. It is also seen that, at the vicinity of the lower surface, $Y \approx 0$, the parameter η_R is larger than zero, therefore, a thermal non-equilibrium region. In contrast, as $Y \rightarrow \infty$, $\eta_R \rightarrow 0$, indicating that rotational and translational temperatures are in thermal equilibrium. Nevertheless, along the lower surface, at sections X of 51, 55 and 100, a different behavior is noticed for η_R profiles. It is noticed that rotational and translational temperatures reach the equilibrium conditions, since $\eta_R \rightarrow 0$ at the vicinity of the back face. In addition, far from the back face and from the flow reattachment point, section $X = 100$, the flow develops again along the surface, and η_R seems to reach the behavior for the flat-plate case.

In order to emphasize the distribution of thermal non-equilibrium associated with rotational temperature, Fig. 4 demonstrates the contour map for η_R at the vicinity of the backward-facing steps defined by height h of 3 and 9 mm. The distribution for h of 6 mm is intermediate to the cases shown, and it will not be presented. According to these plots, the normalized temperature non-equilibrium parameter η_R is larger than zero inside the boundary layer, shock layer and in the expansion region downstream the step corner.

The distribution of non-equilibrium between translational and vibrational temperatures, η_V , is illustrated in Fig. 5 for the same six sections along the upper and lower surfaces of the steps.

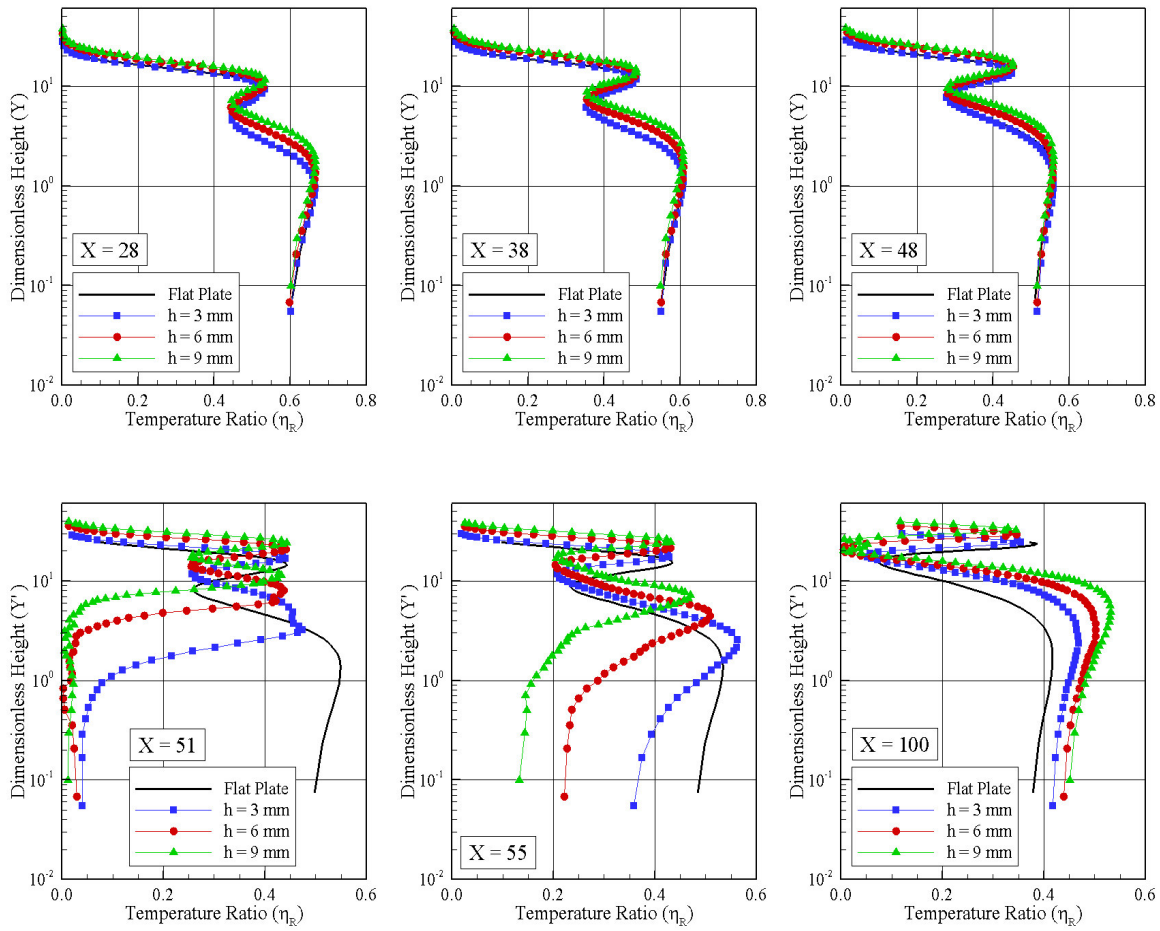


Figure 3: Distribution of η_R profiles along the backward-facing step surface as a function of the height h .

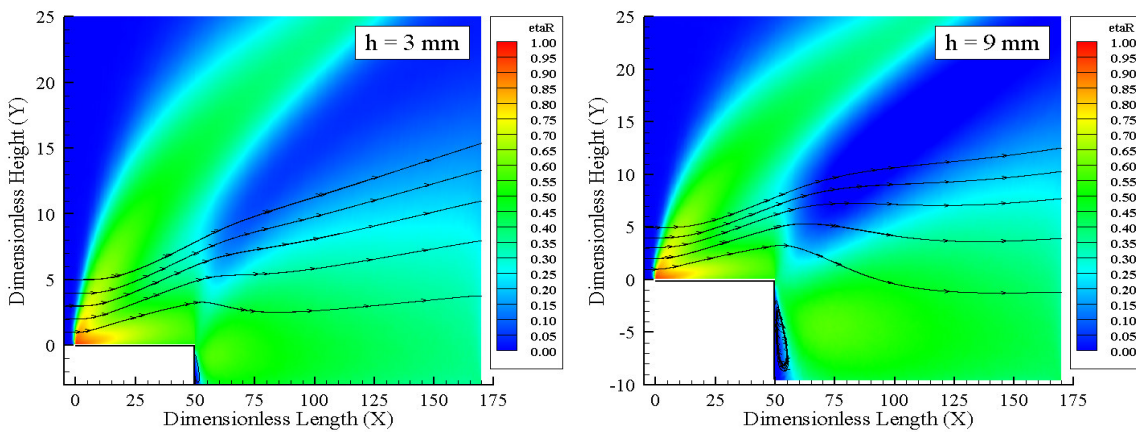


Figure 4: Non-equilibrium between rotational and translational kinetic temperatures, η_R , for a hypersonic flow over backward-facing steps with height h of 3 mm (left) and 9 mm (right).

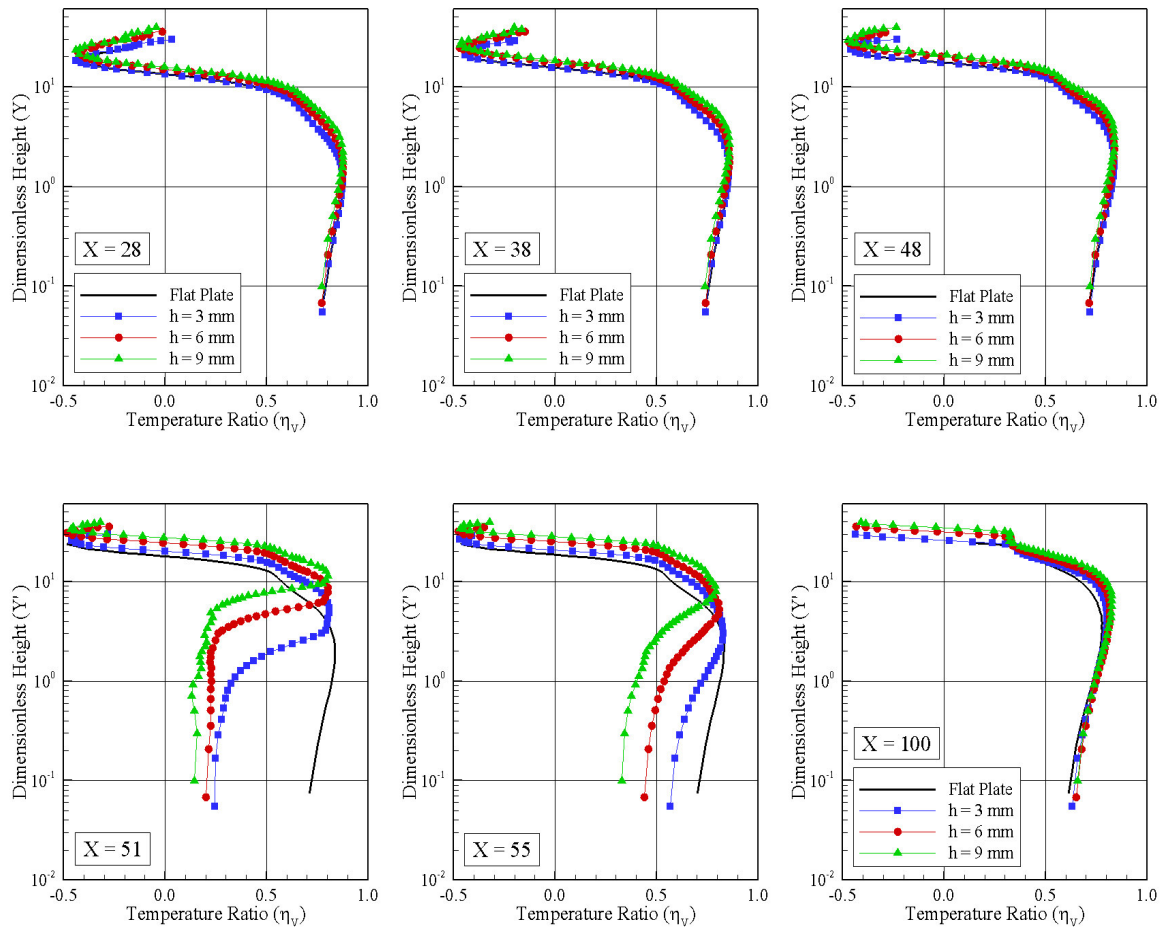


Figure 5: Distribution of η_V profiles along the backward-facing step surface as a function of the height h .

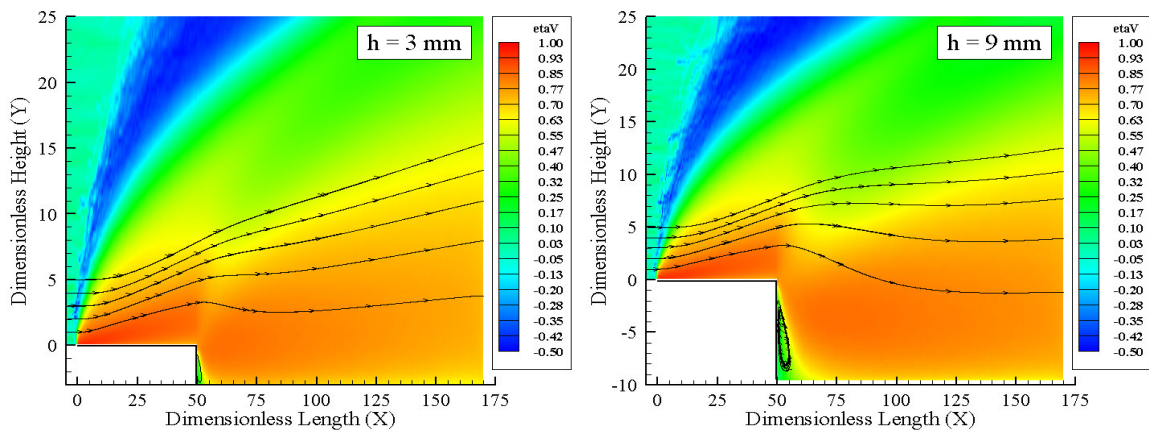


Figure 6: Non-equilibrium between vibrational and translational kinetic temperatures, η_V , for a hyper-sonic flow over backward-facing steps with height h of 3 mm (left) and 9 mm (right).

Based on this set of plots, it is noticed that η_V presents a similar behavior as that demonstrated by η_R in the sense that along the upper surface the profiles follow the same patterns of those for the flat-plate case. In addition, inside the boundary layer and the shock layer, η_V is large showing a high degree of thermal non-equilibrium. Of particular interest is the η_V behavior in the outer part of the shock wave. In this region, $\eta_V < 0$, indicating that the vibrational temperature is slightly larger than the translational temperature. On the other hand, along the lower surface, η_V profiles for the steps differ from those for the flat-plate case, at least close to the back face. Also, it is seen that η_V tends to zero, indicating that the thermal equilibrium is roughly achieved. Moreover, as the flow expands around the step corner and develops along the lower surface, the temperature distribution basically reach the distribution observed for the flat-plate case. In this sense, η_V profiles for the steps are similar to those for the flat-plate case, as shown in the profiles for section $X = 100$.

In an attempt to bring out the essential characteristics of the thermal non-equilibrium associated with vibrational temperature, Fig. 6 displays the contour map for η_V at the vicinity of the backward-facing steps defined by height h of 3 and 9 mm. Similarly to the previous case, the distribution for h of 6 mm will not be presented.

The distribution of non-equilibrium between translational temperature and “parallel” temperature, η_X , along the upper and lower surfaces of the steps is exhibited in Fig. 7. Looking first to the profiles on the upper surface, it may be inferred that the profiles are qualitatively similar to those in Figs. 3 and 5 in the sense that the presence of the steps does not affect the temperature behavior upstream the back faces. Particular attention is paid to the distribution of η_X inside the boundary layer. It is clearly seen that $\eta_X < 1$ in this region, indicating that parallel” temperature T_X is larger than the translational temperature T_T . An understanding of this behavior can be gained by analyzing Eqs. (10), (11) and (12). Turning to the profiles on the lower surface, a different behavior is seen for η_X profiles close to the back faces. It is seen that η_X approaches zero for section $X = 51$. This is an expected behavior since the flow is roughly in thermal equilibrium, as was pointed earlier. In what follows, at section $X = 100$, η_X increases negatively and reaches the values attained by the flat-plate case. In addition, it may be recognized from this set of plots that η_X profiles for section $X = 100$ is very similar to those at section $X = 48$, an indication that the flow is recovering that ones observed for the flat-plate case.

In an effort to emphasize interesting features of the thermal non-equilibrium associated with kinetic temperature based on the velocity component in the x -direction, Fig. 8 demonstrates contour maps for η_X at the vicinity of the backward-facing steps defined by height h of 3 and 9 mm. Contour maps for the whole flowfield confirm thermal non-equilibrium in the boundary layer and inside the shock layer.

The distribution of non-equilibrium between translational temperature and “normal” temperature, η_Y , is depicted in Fig. 9 for a total of six sections along the upper and lower surfaces of the steps. On examining the η_Y profiles along the upper surface, it is observed that they are similar to η_X profiles in the sense that they basically follow the same patterns of those presented for the flat-plate case. On the other hand, they differ from those for η_X in the sense that $\eta_Y > 1$ inside the boundary layer, while $\eta_X < 1$. Therefore, for this particular region, “normal” temperature T_Y is smaller than the translational temperature, while “parallel” temperature T_X is larger than the translational temperature T_T . It should be mentioned in this context that the temperature T_X , based on the velocity component in the x -direction, is larger than the temperature T_Y , based on the velocity component in the y -direction. The reason for that is because the velocity difference between the two groups of molecules in the shock wave, related to the near bimodal distribution mentioned earlier, is basically along the x -axis.

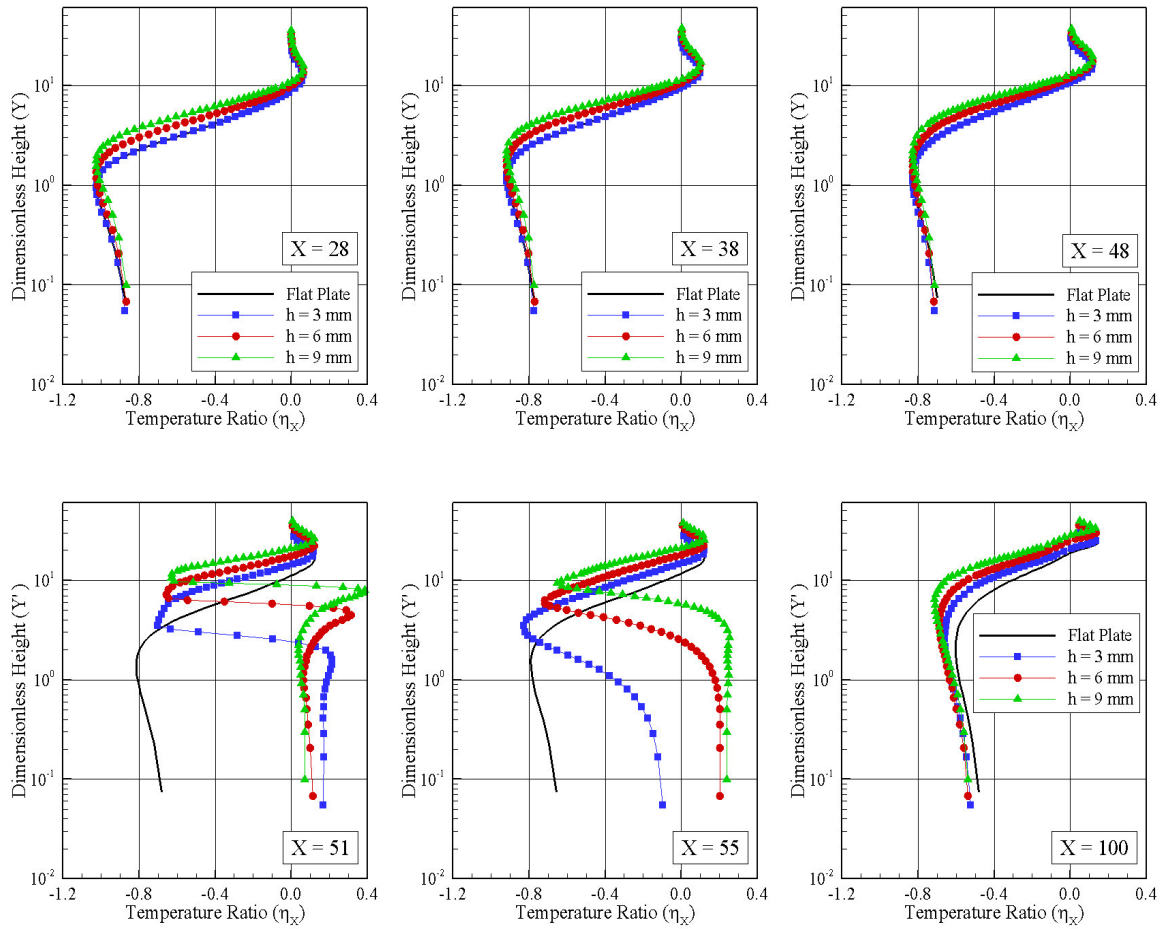


Figure 7: Distribution of η_X profiles along the backward-facing step surface as a function of the height h .

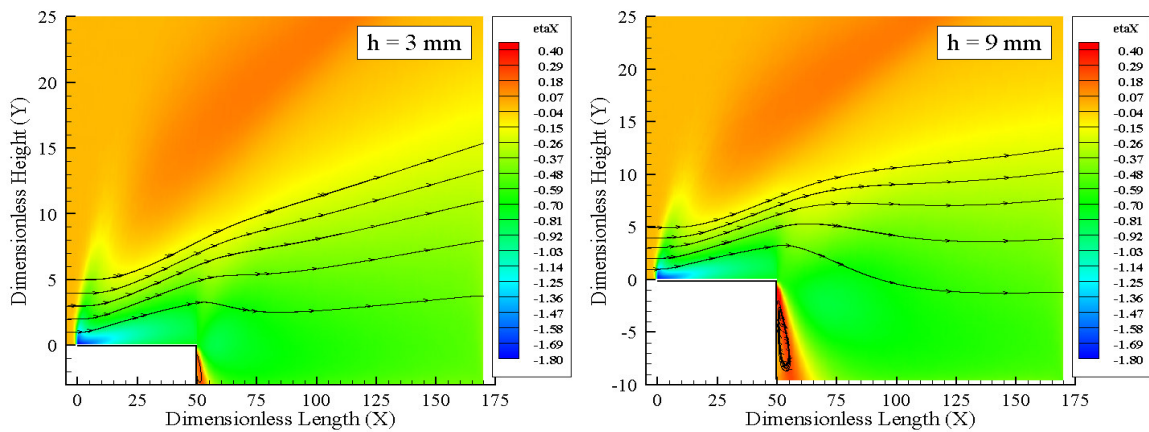


Figure 8: Non-equilibrium between “parallel” and translational kinetic temperatures, η_X , for a hypersonic flow over backward-facing steps with height h of 3 mm (left) and 9 mm (right).

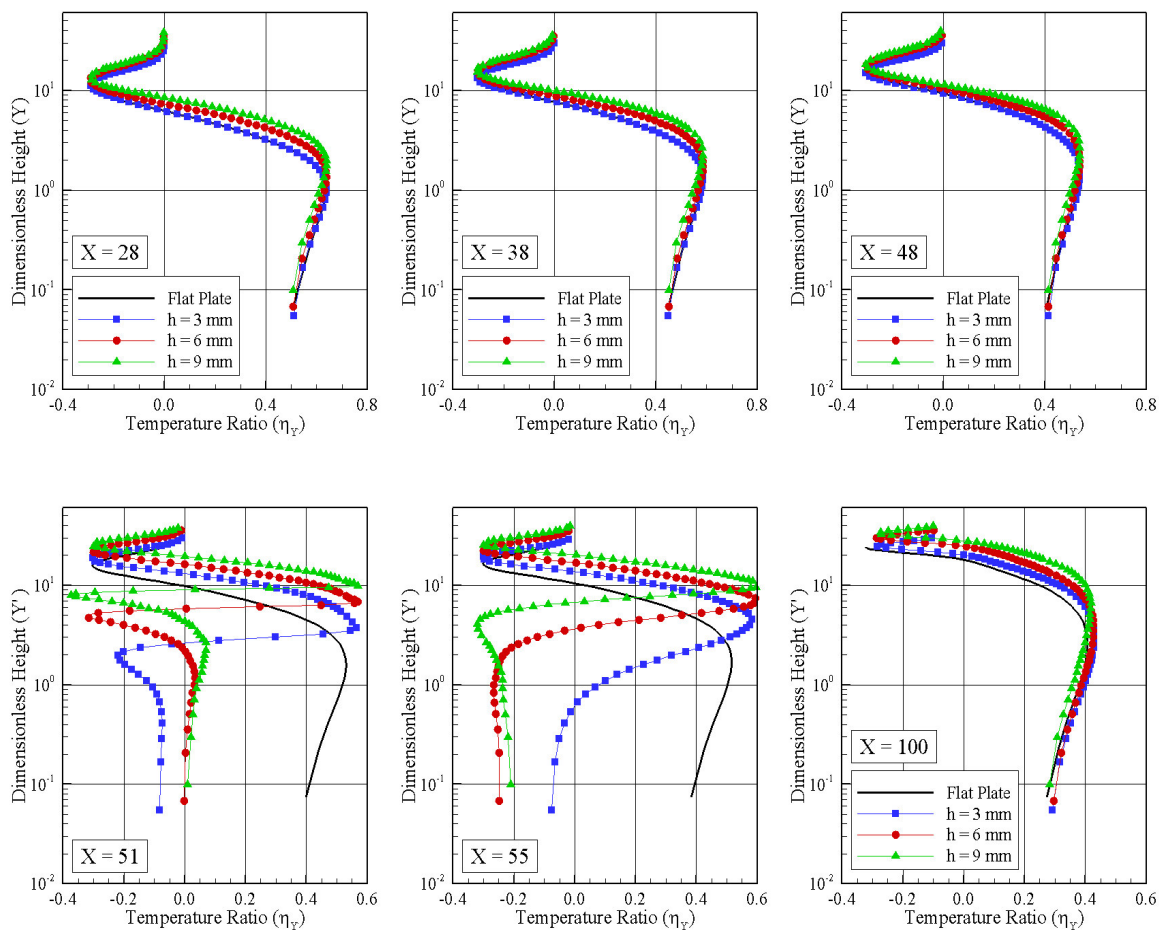


Figure 9: Distribution of η_T profiles along the backward-facing step surface as a function of the height h .

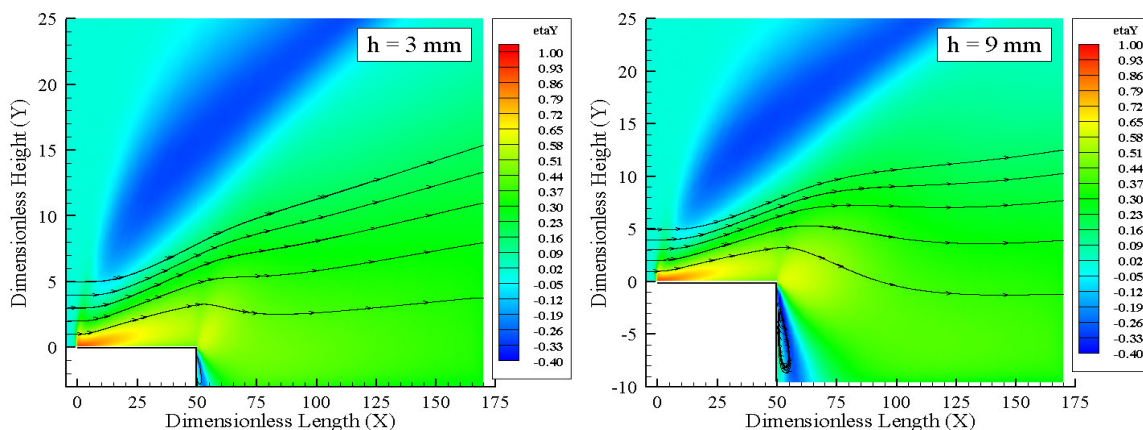


Figure 10: Non-equilibrium between “normal” and translational kinetic temperatures, η_Y , for a hypersonic flow over backward-facing steps with height h of 3 mm (left) and 9 mm (right).

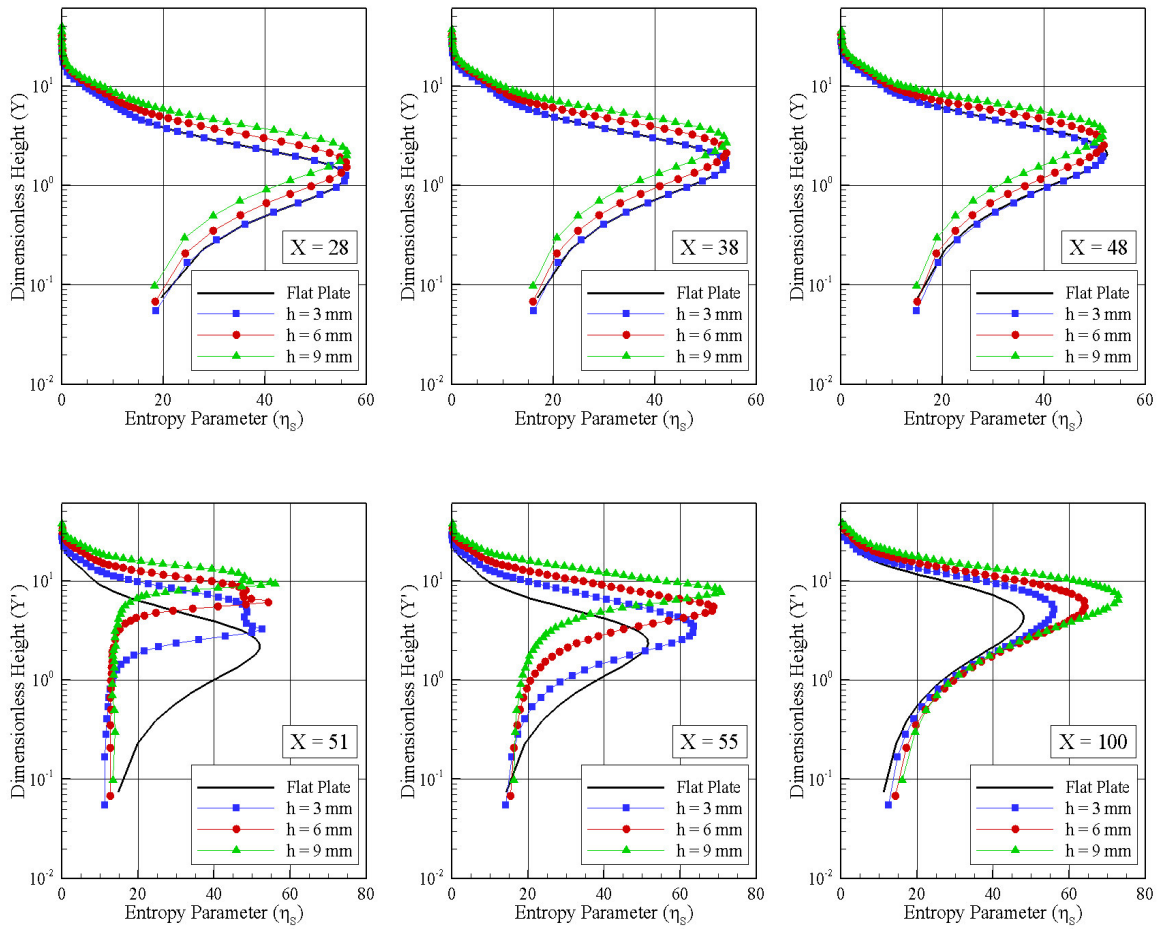


Figure 11: Distribution of η_S profiles along the backward-facing step surface as a function of the height h .

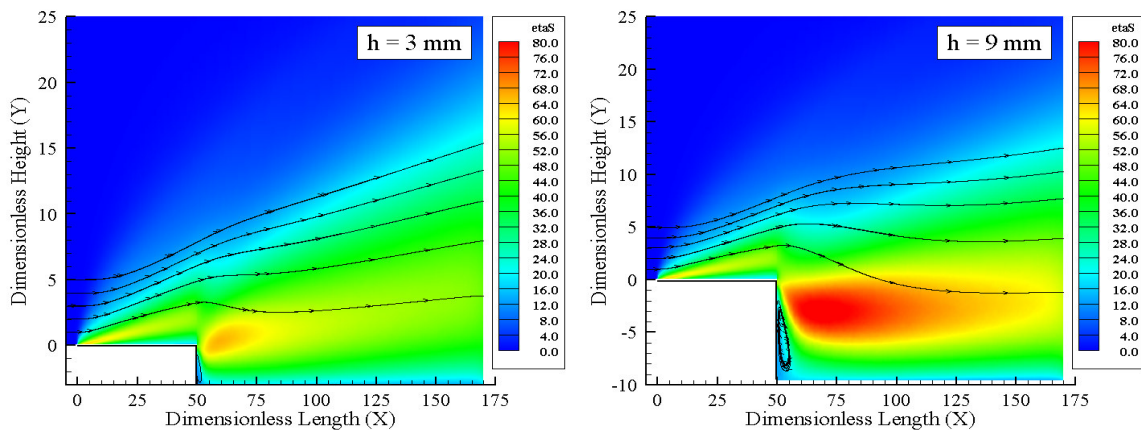


Figure 12: Contour map for entropy parameter, η_S , for a hypersonic flow over backward-facing steps with height h of 3 mm (left) and 9 mm (right).

In the following, Fig. 10 illustrates contour maps for thermal non-equilibrium associated with kinetic temperature based on the velocity component in the y -direction, η_Y , at the vicinity of the backward-facing steps defined by height h of 3 and 9 mm. Again, contour maps for the whole flowfield confirm thermal non-equilibrium inside the boundary layer and the shock layer.

Having a clear qualitative picture of the flow patterns associated with the thermal non-equilibrium between rotational, vibrational, “parallel”, “normal”, and translational temperatures, it proves convenient to assess the overall performance of entropy. In this fashion, an entropy parameter is defined as follows,

$$\eta_S = \frac{p/p_\infty}{(\rho/\rho_\infty)^\gamma} - 1 \quad (13)$$

where γ is the specific heat ratio.

It is very encouraging to observe that, for the present DSMC simulations, the specific heat ratio γ depends on the temperature, and is related to the number of excited degrees of freedom ζ for translation, rotation and vibration by the following equation,

$$\gamma = \frac{\zeta_T + \zeta_R + \zeta_V + 2}{\zeta_T + \zeta_R + \zeta_V} \quad (14)$$

where subscripts T , R and V stand for translation, rotation and vibration, respectively.

Figure 11 displays the η_S profiles for the same six sections along the upper and lower surfaces presented previously, and for completeness, Fig. 12 demonstrates the entropy contours in the flow along with some typical streamlines around the backward-facing steps defined by height h of 3 and 9 mm. According to these plots, the entropy generation is positive due to the flow compression through the shock wave. It is observed that in the region near to the upstream boundary, at the vicinity of sharp leading edge, the entropy parameter η_S approaches zero, i.e., the flow is basically isentropic, as would be expected.

5. CONCLUDING REMARKS

In the current study, a rarefied hypersonic flow over backward-facing steps has been investigated by using the Direct Simulation Monte Carlo (DSMC) method. The simulations provided information concerning the nature of the thermal non-equilibrium effects in the flowfield around the steps. The effect of non-equilibrium between rotational temperature, vibrational temperature, “parallel” temperature, “normal” temperature, and translational temperature was investigated for back-face height h of 3, 6 and 9 mm, which corresponded to Knudsen numbers in the transition flow regime.

According to the simulations, a thermal non-equilibrium flow was found inside the boundary layer and the shock layer. It was also found that, at the vicinity of the back faces, the flow is roughly in thermal equilibrium. In this region, rotational temperature, vibrational temperature, “parallel” temperature, and “normal” temperature, basically reach the same value observed for the translational temperature.

6. ACKNOWLEDGEMENTS

The authors would like to thank the financial support provided by CNPq (Conselho Nacional de Desenvolvimento Científico e Tecnológico) under Grant No. 473267/2008-0.

REFERENCES

- Alexander, F. J., Garcia, A. L., and Alder, B. J., Cell size dependence of transport coefficient in stochastic particle algorithms. *Physics of Fluids*, 10:1540–1542, 1998.
- Alexander, F. J., Garcia, A. L., and Alder, B. J., Erratum: Cell size dependence of transport coefficient in stochastic particle algorithms. *Physics of Fluids*, 12:731–731, 2000.
- Bejan, A., Advanced engineering thermodynamics. John Wiley and Sons, 1988.
- Bird, G. A., Monte Carlo simulation in an engineering context. *Progress in Astronautics and Aeronautics: Rarefied gas Dynamics*, ed., Fisher, S. S., AIAA New York, 74:239–255, 1981.
- Bird, G. A., Perception of numerical method in rarefied gasdynamics. *Rarefied Gas Dynamics: Theoretical and Computational Techniques*, Progress in Astronautics and Aeronautics, eds. Muntz, E. P., Weaver, D. P. and Capbell, D. H., AIAA, New York, 118:374–395, 1989.
- Bird, G. A., *Molecular gas dynamics and the direct simulation of gas flows*, Oxford University Press, 1994.
- Borgnakke, C. and Larsen, P. S., Statistical collision model for Monte Carlo simulation of polyatomic gas mixture. *Journal of Computational Physics*, 18:405–420, 1975.
- Charwat, A. F., Dewey, C. F., Roos, J. N. and Hitz, J. A., An investigation of separated flows. 1: The pressure field. *Journal of aerospace Sciences*, 28:457–470, 1961.
- Donaldson, I. S., On the separation of a supersonic flow at a sharp corner. *AIAA Journal*, 5:1086–1088, 1967.
- Gai, S.L., and Milthorpe, J. F., Hypersonic high-enthalpy flow over a blunt-stepped cone. *Proceedings of the 20th International Symposium on Shock Waves*, 234–244, 1995.
- Gai, S. L., Reynolds, C. R., and Baird, J. P., Measurements of heat transfer in separated high-enthalpy dissociated laminar hypersonic flow behind a step. *Journal of Fluid Mechanics*, 199:541–561, 1989.
- Garcia, A. L., and Wagner, W., Time step truncation error in direct simulation Monte Carlo. *Physics of Fluids*, 12:2621–2633, 2000.
- Grotowsky, M. G., and Ballmann, J., Numerical investigation of hypersonic step-flows. *Shock Waves*, 10:57–72, 2000.
- Hadjiconstantinou, N. G., Analysis of discretization in the direct simulation Monte Carlo. *Physics of Fluids*, 12:2634–2638, 2000.
- Leite, P. H. M., Direct simulation of the step influence on a reentry vehicle surface (in Portuguese). MS Dissertation, INPE, 2009.
- Leite, P. H. M., and Santos, W. F. N., Direct simulation calculations of the rarefied hypersonic flow past a backward-facing step. *2009 Brazilian Symposium on Aerospace Engineering and Applications*, São José dos Campos, SP, Brazil, 2009a.
- Leite, P. H. M., and Santos, W. F. N., Direction simulation of heat transfer and pressure distributions of hypersonic flow over backward-Facing Steps. XII Encontro de Modelagem Computacional, Rio de Janeiro, RJ, Brazil, 2009b.
- Liepmann, H. W., Narasimha, R. and Chahine, M., Theoretical and experimental aspects of the shock structure problem. *Proceedings of the 11th International Congress of Applied Mechanics*, edited by H. Gortler, Munich, Germany, 973–979, 1964.
- Loth, E., Kailasanath, K., and Löhner, R., Supersonic flow over an axisymmetric backward-facing step. *Journal of Spacecraft and Rockets*, 29:352–359, 1992.
- Mates, R. E., and Weatherston, R. C., Definition of temperature in nonequilibrium process. *Physics of Fluids*, 8:657–662, 1965.
- Rom, J., and Seginer, A., Laminar heat transfer to a two-dimensional backward facing step from the high-enthalpy supersonic flow in the shock tube. *AIAA Journal*, 2:251–255, 1964.

- Schaff, S. and Chambre P., *Fundamentals of gas dynamics*. Princeton University Press, Princeton, NJ, 1958.
- Scherberg, M. G., and Smith, H. E., An Experimental study of supersonic flow over a rearward facing step. *AIAA Journal*, 5:51–56, 1967.
- Shang, J. S., and Korkegi, R. H., Investigation of flow separation over a rearward-facing step in a hypersonic stream. *AIAA Journal*, 6:986–987, 1968.